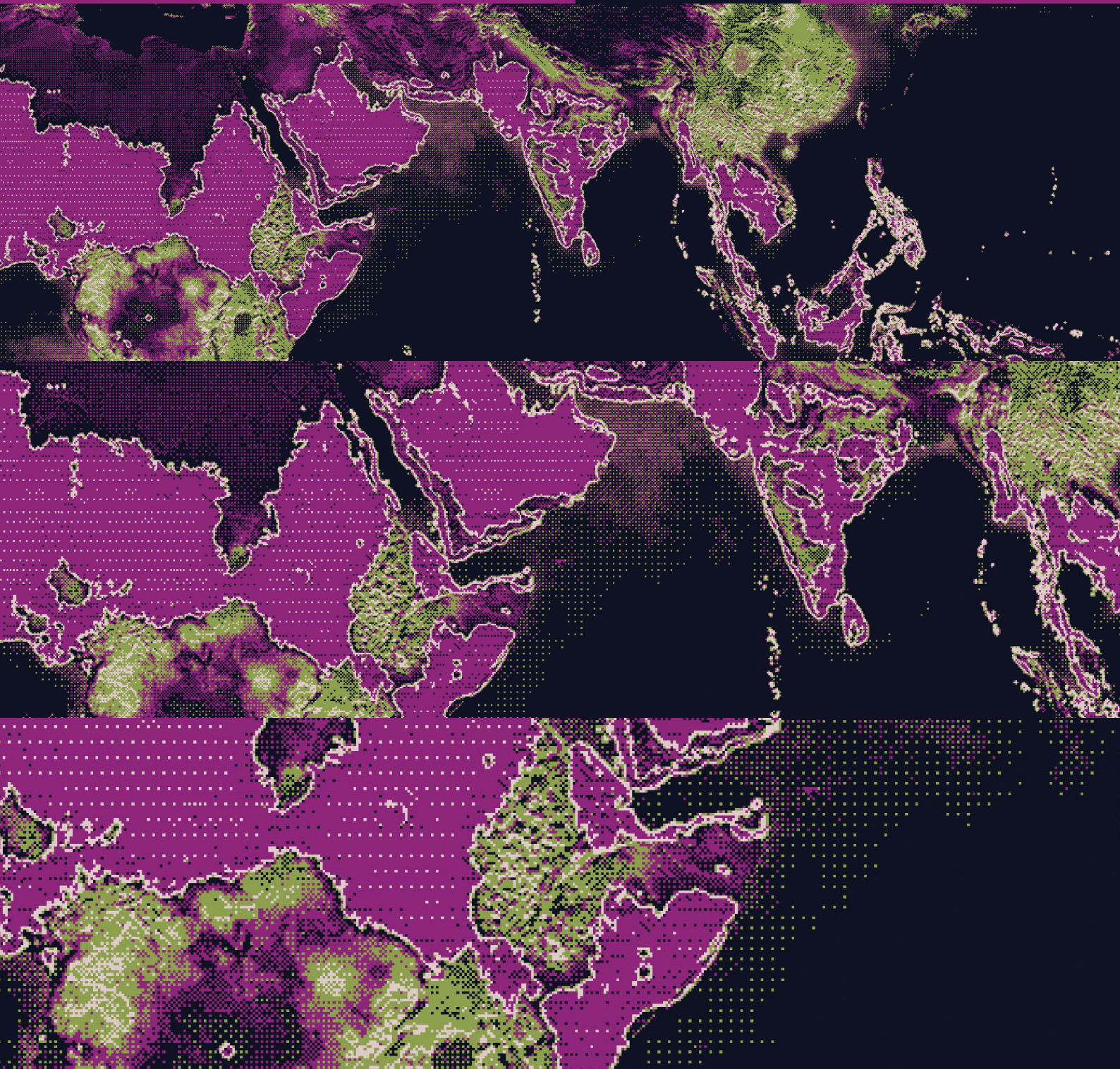


*RADICAL
ECOLOGY*



**Quantifying
the human cost
of global warming**

Against Apartheid

Our new study on projected movement in the human climate niche locates the origins of delayism in historic usage of the climate and economic model and puts forward a bold new approach for quantifying the human cost of global warming that could drive a sea-change in policy and justice.

In February 2022, as we were pulling together the first drafts of the paper, *Quantifying the Human Cost of Global Warming*, the White House Office of Science and Technology Policy [OSTP] brought together a virtual roundtable of natural and social scientists to “discuss the scientific understanding of why arguments for delaying climate action are appealing and how they can be countered effectively”.

Then Head of OSTP and Deputy Assistant to the US President, Dr Alondra Nelson, opened the meeting by referencing “forces hostile to climate action - running the gamut from self-interest and short-term thinking, to deliberate disinformation campaigns that are as insidious as they are invidious”.

COP26 had failed to move things beyond a situation where global warming is projected to exceed 2.7°C by the end of the century and COP27 witnessed no significant advance on this scenario either while, according to a report published in December by Christian Aid, 2022 saw a spate of extreme weather events in which 10 climate disasters cost more than \$3 billion USD each.

The costliest in financial terms, Hurricane Ian, incurred damages across the USA and Cuba in excess of \$100 billion USD whilst, in human terms, the Pakistan floods killed more than 1700 people, displaced more than 7 million and drove up to 15 million people into poverty, according to World Bank estimates.

Global commitments on climate finance, however, continue to fall short of the \$100 billion/year promised by the world’s richest nations in Copenhagen in 2009, indicating a growing deficit that continues to push the escalating burden of climate impacts onto those who are most vulnerable and least responsible for causing climate change.

The question of how best to quantify this rising inequality in order to strengthen future policymaking has been at the forefront of our thinking whilst conducting this study.

Pakistan, for example, the eighth most climate vulnerable country in the world, according to the Global Climate Risk Index, is responsible for around 0.3% of all greenhouse gas emissions (as compared with the USA at 24.2%). The 2022 floods there incurred economic damages, according to the World Bank, of around \$30 billion USD but the country was able to access only \$5.6 billion USD in insurance payments and \$9 billion USD in international aid.

Pakistan’s own reserves total just \$4.5 billion USD and as of 9 May 2023, the credit ratings agency, Moody’s Investor Service, identified the country as being at risk of defaulting on existing debt payments without the intervention of an IMF bailout that to-date has not been agreed.

The scenario points towards what UN Special Rapporteur Philip Alston described, presenting his 2019 report on climate change and poverty, as a coming “climate apartheid”, “where the wealthy pay to escape overheating, hunger and conflict while the rest are left to suffer”.

Quantifying the Human Cost of Global Warming responds at the level of the climate model by acknowledging, first, how systems that have underpinned the economics of climate change and guided policy and government decision-making have often reinforced this dynamic by (1.) emphasising the projected cost of climate change in monetary and not primarily human terms, (2.) therefore placing a greater value on climate impacts suffered by the rich than the poor and (3.) placing greater value on current over future generations (because future damages are subject to economic discounting).

2018 Nobel Prize Winner, William Nordhaus’s DICE model, which continues to exert a dominant influence, is exemplary of this approach. Having evolved through successive iterations since the 1990s, it has driven the quest to establish appropriate figures for the social cost of carbon, most notably in the US since the time of the Obama administration.

Yet the 2007-DICE model, by placing greater value on centres of wealth than on human suffering, calculated the social cost of reducing carbon emissions in line with 1.5°C targets as being more than \$1 trillion USD greater than the cost of taking no action at all, whilst the 2016-DICE model calculated that an optimal carbon tax would limit global warming to 3.5°C not 2.5°C by the year 2100.

In both scenarios we are presented with figures that gravely underestimate the human costs of climate breakdown, invisibilising victims of climate impacts in a way that would encourage any company board or cabinet body to think twice before ruling out an approach to climate action that took its time.

This delayism, that has become an orthodoxy of contemporary climate governance and its crisis of inaction, in many ways derives from this use of the model that has encouraged us to see the world and our future in this way.

By contrast, our approach to the quantification of climate impacts starts out from the principle that the lives of all humans, whether rich or poor, young or old, should be valued equally and this approach yields radically different numbers and a very different perspective on the value of urgent action when faced with the crisis of global warming.

By comparing projected movement in the human climate niche with movement in the global population, we have found that the projected rise of 2.7°C by 2100, for example, (the likely outcome of existing policy commitments) stands to leave two billion people – more than one fifth of humanity – exposed to dangerous levels of heat (in a situation where around 60 million people are already exposed in this way).

In this scenario, limiting warming to 1.5°C would leave only 5% of the human population exposed, saving a sixth of humanity compared with warming of 2.7°C, while the worst-case/no-action scenarios of 3.6°C or even 4.4°C global warming could put half of the world’s population outside the human climate niche, posing an “existential threat”.

Clearly, these metrics do not lead us to conclusions that no action would be in any way cost-beneficial compared to limiting global warming to 1.5°C. Instead they underline the enormous value of early and decisive action to reduce carbon emissions whilst also pointing us towards the profound inequalities that characterise the distribution of both impacts and responsibility for causing climate change that will also need to be addressed in the design of collective solutions.

Of the two billion people displaced outside the human climate niche at 2.7°C, for example, more than 600 million of them are projected to be in India and more than 300 million in Nigeria in a situation where per capita emissions in these countries are less than half the global average.

The inequality remains as stark when considered in relation to future generations since we find that 3.5 global average citizens and 1.2 average US citizens currently emit enough carbon in their lifetimes to expose one future person, a person who is statistically most likely to be black or brown, to unprecedented heat. In the words of the poet, June Jordan, “it would be something fine if we could learn how to bless the lives of children.”

Quantifying the human cost of global warming

This paper was published in *Nature Sustainability* on 22 May 2023:

Lenton, T.M., Xu, C., Abrams, J.F. *et al.* Quantifying the human cost of global warming. *Nat Sustain* 6, 1237–1247 (2023).

Despite increased pledges and targets to tackle climate change, current policies still leave the world on course for around 2.7°C end-of-century global warming^{1,2,3,4,5} above pre-industrial levels—far from the ambitious aim of the Paris Agreement to limit global warming to 1.5°C. Even fully implementing all 2030 nationally determined contributions, long-term pledges and net zero targets, nearly 2°C global warming is expected later this century^{1,2,5}. Calls for climate justice highlight the vital need to address the social injustices driven by climate change⁶. But what is the human cost of climate change and who bears it? Existing estimates tend to be expressed in monetary terms⁷, tend to recognize impacts on the rich more than those on the poor (because the rich have more money to lose) and tend to value those living now over those living in the future (because future damages are subject to economic discounting). From an equity standpoint, this is unethical⁸—when life or health are at stake, all people should be considered equal, whether rich or poor, alive or yet to be born.

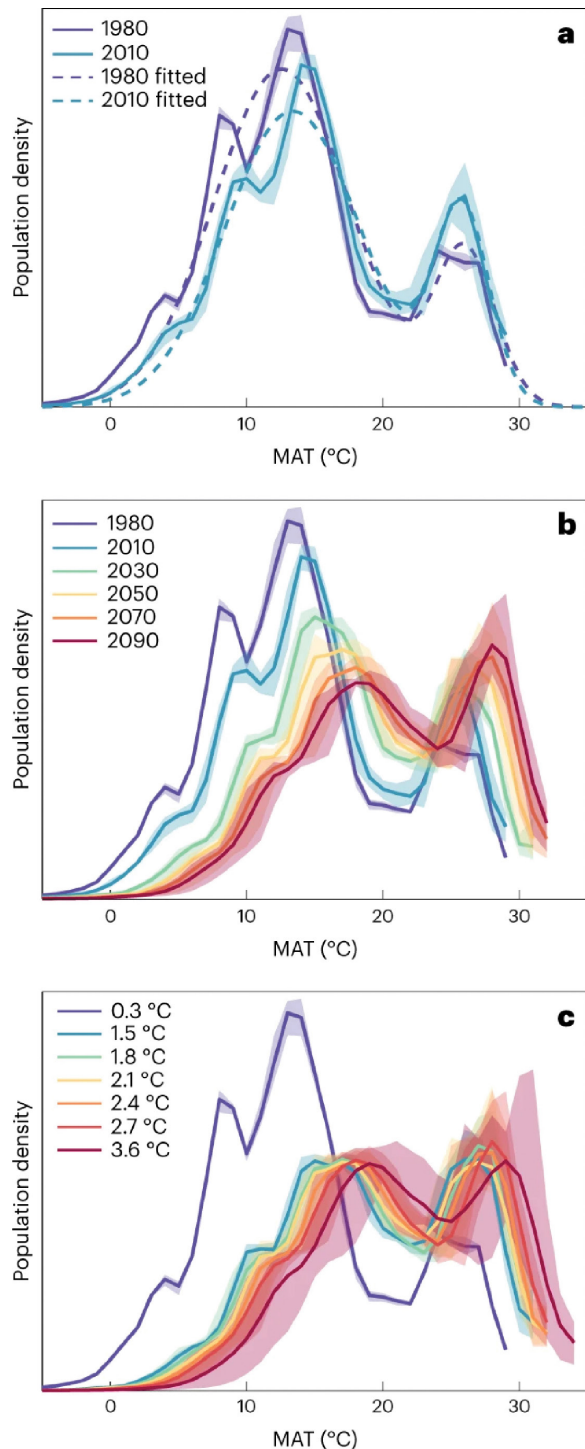
A growing body of work considers how climate variability and climate change affect morbidity⁹ or mortality^{10,11,12,13}. Here, we take a complementary, ecological approach, considering exposure to less favourable climate conditions, defined as deviations of human population density with respect to climate from the historically highly conserved distribution—the ‘human climate niche’¹⁴. The climate niche of species integrates multiple causal factors including combined¹⁵ effects of physiology¹⁶ and ecology¹⁷. Humans have adapted physiologically and culturally to a wide range of local climates, but despite this our niche¹⁴ shows a primary peak of population density at a mean annual temperature (MAT) of ~13°C and a secondary peak at ~27°C (associated with monsoon climates principally in South Asia). The density of domesticated crops and livestock follow similar distributions¹⁴, as does gross domestic product, which shares the same independently identified^{14,18} primary temperature peak (~13°C). Mortality also increases at both high and low temperatures^{10,11,12}, consistent with the existence of a niche.

Here, we reassess the human climate niche, review its mechanistic basis, link it to temperature extremes, and calculate exposure outside the niche up to present and into the future under different demographic scenarios and levels of global warming. Exposure outside the niche could result in increased morbidity, mortality, adaptation in place or displacement (migration elsewhere). High temperatures have been linked to increased mortality^{12,13}, decreased labour productivity¹⁹, decreased cognitive performance²⁰, impaired learning²¹, adverse pregnancy outcomes²², decreased crop yield potential⁹, increased conflict^{23,24,25}, hate speech²⁶, migration²⁷ and infectious disease spread^{9,28,29}. Climate-related sources of harm not captured by the niche include sea-level rise^{30,31}.

Reassessing the niche

First, we re-examined how relative population density varies with MAT. Our previous work¹⁴ considered the 2015 population distribution under the 1960–1990 mean climate as a baseline (Extended Data Fig. 1). Here, we use the 1980 population distribution (total 4.4 billion) under the 1960–1990 mean climate (Fig. 1a; ‘1980’) as the reference state. This is a more internally consistent approach, particularly as recent population growth biases towards hotter places. Applying a double-Gaussian fitting, the primary temperature peak is now larger and at a slightly lower temperature (~12 °C), in better agreement with reconstructions from 300, 500 and 6,000 years BP (Extended Data Fig. 1). The 1960–1990 interval was globally ~0.3 °C warmer than the 1850–1900 ‘pre-industrial’ level, but closer to mean Holocene temperatures that supported civilizations as we know them (because 1850–1900 was at the end of the Little Ice Age). The smoothed double-Gaussian function fit (Fig. 1a; ‘1980 fitted’) is referred to from hereon as the ‘temperature niche’. An updated ‘temperature–precipitation niche’ (additionally considering mean annual precipitation; MAP) was also calculated and considered in sensitivity analyses. It shows a marked drop in population density^{14,32} below 1,000 mm yr^{−1} MAP. The temperature niche captures a key part of this effect because its minimum at 19–24 °C is associated with dry subtropical climates (Extended Data Fig. 2). However, the temperature niche overestimates population density at very low MAP (notably in temperate deserts) and at high MAP (Supplementary Fig. 1). Hence, projections with the temperature niche are more conservative than those with the temperature–precipitation niche. By either definition, the niche is largely that of people dependent on farming. The niche of hunter-gatherers is probably broader^{33,34,35,36}, as it is not constrained by the niches of domesticated species. This hypothesis is supported by the broader distribution of population density with respect to temperature reconstructed¹⁴ from the ArchaeoGLOBE dataset for 6,000 years BP (when a smaller fraction of total population depended on farming; Extended Data Fig. 1b).

Fig. 1: Changes in relative human population density with respect to MAT.



a, Observed changes from the reference distribution for 1980 population (4.4 billion) under 1960–1990 climate (0.3 °C global warming), to the 2010 population (6.9 billion) under 2000–2020 climate (1.0 °C global warming), together with smooth fitted functions ('1980 fitted' is defined as the temperature niche).

b, Observed and projected future changes in population density with respect to MAT following SSP2-4.5 leading to ~2.7 °C global warming and peak population 9.5 billion (see Extended Data Table 1 for global warming and population levels at each time).

c, Projected population density with respect to MAT for a future world of 9.5 billion people under different levels of global warming (1.5, 1.8, 2.1, 2.4, 2.7 and 3.6 °C), contrasted with the reference distribution (0.3 °C, 1980 population). Data are presented as mean values with the shaded regions corresponding to 5th–95th percentiles.

Mechanisms behind the niche

The human climate niche is shaped by direct effects of climate on us and indirect effects on the species and resources that sustain or afflict us. Direct climate effects include health impacts and changes in behaviour. Human perceptions of thermal comfort evolved³⁷ to keep us near optimal conditions of 22–26°C, with well-being declining³⁸ above 28°C. Behavioural changes include altering clothing, changing environment (including to indoor environments) and altering work patterns³⁹. These can buffer individual exposure to temperature extremes but still affect collective well-being via effects on work. Sometimes uncomfortable conditions are unavoidable. High temperatures can decrease labour productivity¹⁹, cognitive performance²⁰ and learning²¹, produce adverse pregnancy outcomes²², and increase mortality^{10,11,12}. Exposure to temperatures $>40^\circ\text{C}$ can be lethal⁴⁰, and lethal temperature decreases as humidity increases^{12,40}. At wet-bulb temperature (WBT) $>28^\circ\text{C}$, the effectiveness of sweating in cooling the body decreases, and WBT $\sim 35^\circ\text{C}$ can be fatal^{41,42} especially for more vulnerable individuals⁴³ (as the body can no longer cool itself). High temperatures can also trigger conflict^{23,24,25} or migration²⁷ to lower temperature locations.

Indirect effects of climate occur where climate influences the distribution and abundance of species or resources that sustain or afflict humans. Warmer, wetter conditions tend to favour vectors of human disease^{9,28,29,44}. The majority of the world's population remains directly dependent on access to freshwater and lives within 3 km of a surface freshwater body^{14,32,45}. Around 2 billion people depend on subsistence agriculture and thus the climate niche(s) of their crops. A further 120 million pastoralists depend on their domesticated animals, which as mammals have similar physiological limits to humans^{40,46}. Despite a globalized food market, most countries pursue food security through localized production. This couples the rest of us to the climate niches of the crops and livestock we consume, which are similar to the niche of humans¹⁴. High temperatures decrease crop yield potential⁹ and warming is spreading key crop pests and pathogens^{47,48}. Major rainfed crops (maize, rice, wheat) are already migrating⁴⁹, somewhat mitigated by increases in irrigation⁴⁹. This and the historical constancy of the niche (Extended Data Fig. 1a) suggest technological advancement has limited potential to expand the human climate niche in future.

Calculating exposure

For projections, we assume the temperature niche remains unaltered, and provide three calculations of exposure outside of it: (1) exposure to unpreceded heat; (2) total exposure due to temperature change only; or (3) total exposure due to temperature and demographic change (see Methods). (1) The simplest approach¹⁴ just considers 'hot exposure'—that is, how many people fall outside the hot edge of the temperature niche. This is calculated¹⁴ for a given climate and population distribution as the percentage of population exposed to MAT $\geq 29^\circ\text{C}$, given that only 0.3% of the 1980 population (12 million) experienced such conditions in the 1960–1990 climate. (2) Total exposure due to temperature change alone¹⁴ considers all areas where temperature increases to a value supporting lower relative population density according to the temperature niche. To calculate this¹⁴ (Extended Data Fig. 3), we apply the niche to create a spatial 'ideal distribution' of relative population density under a changed climate that maintains the historical distribution with respect to temperature. This is contrasted with the spatial 'reference distribution' of population density with respect to the 1960–1990 climate. The difference between the two distributions integrated across space gives the percentage of population exposed outside the niche due to climate only. (3) Demographic change can also expose an increased density of population to a less favourable climate. To provide an upper estimate of population exposure (in %) due to both temperature and demographic change (Extended Data Fig. 3), we integrate the difference between the projected spatial 'assumed distribution' of population density with respect to temperature and the 'ideal distribution'.

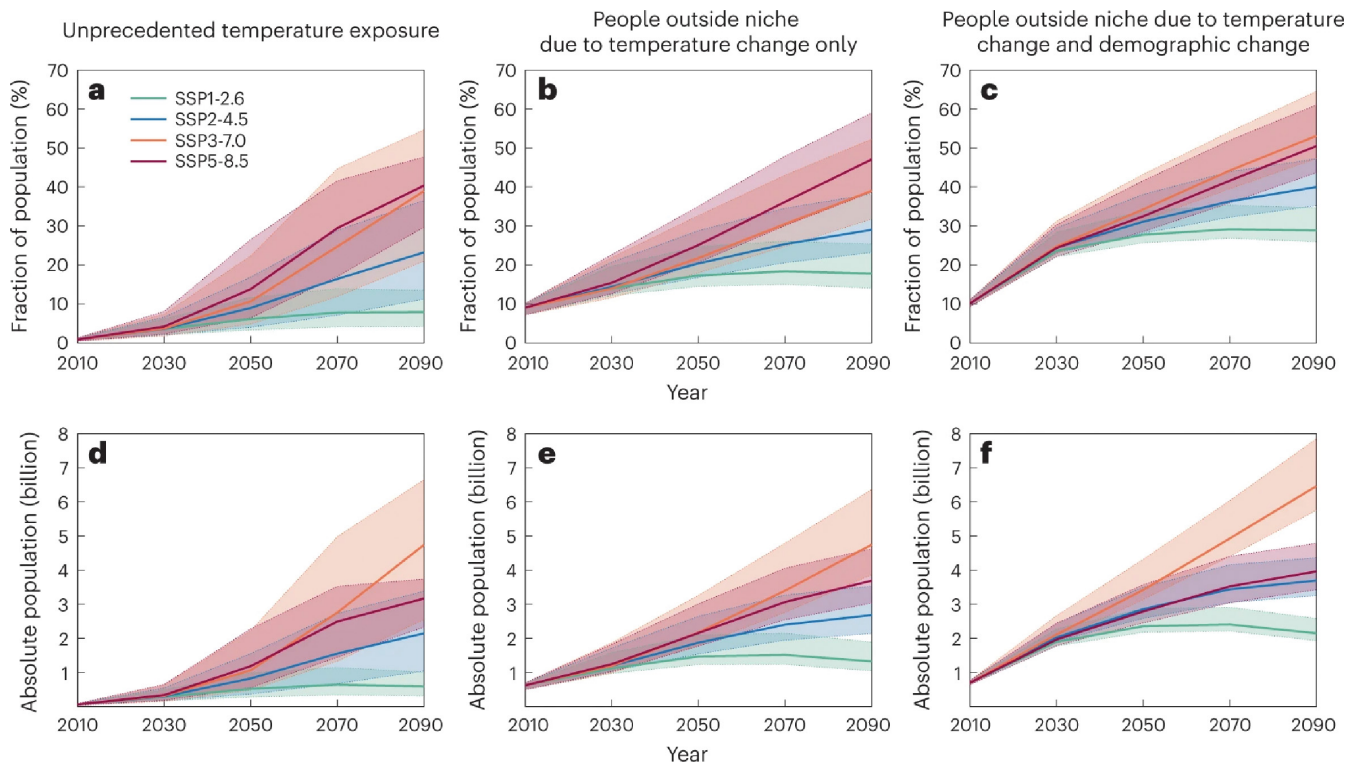
Linking average temperature to other thermal metrics

MAT has the advantage of data availability for characterizing and projecting the human climate niche—it can be easily derived from observational data, reanalysis or climate model output. However, other metrics with less available data have been proposed to better capture thermal tolerance of humans, including mean maximum temperature⁴⁶ (MMT) and WBT⁴⁰. Reassuringly, we find that MAT is very highly correlated with both annual MMT and mean annual WBT (Supplementary Fig. 2). Given the importance of extremes, we also considered how the number of days with maximum temperature $>40^{\circ}\text{C}$ or with WBT $>28^{\circ}\text{C}$ varies with MAT (Extended Data Fig. 4). Potentially lethal⁴⁰ exposure to maximum temperature $>40^{\circ}\text{C}$ starts to increase markedly above MAT $\sim 27^{\circ}\text{C}$, reaching an average of over 75 days a year at MAT $\sim 29^{\circ}\text{C}$ (half the longest time experienced in the present world), and almost all locations with MAT $\geq 29^{\circ}\text{C}$ experience a substantial number of days with maximum temperature $>40^{\circ}\text{C}$ (Extended Data Fig. 4a). Physiologically challenging exposure to WBT $>28^{\circ}\text{C}$ starts to increase at MAT $>22^{\circ}\text{C}$ and exceeds an average of 10 days per year at MAT $\geq 29^{\circ}\text{C}$ (Extended Data Fig. 4b). Together these results show that MAT provides a good proxy for characterizing thermal tolerance, with MAT $\geq 29^{\circ}\text{C}$ providing a reasonable measure of unprecedented heat exposure, although it does not capture all exposure to temperature extremes.

Changes up to present

We find that noticeable changes in the distribution of population density with respect to temperature have occurred due to temperature and demographic changes from 1980 to 2010 (Fig. 1a). Considering the 2010 population distribution (total 6.9 billion) under the observed 2000–2020 climate, global warming of 1.0°C (0.7°C above 1960–1990) has shifted the primary peak of population density to a slightly higher temperature ($\sim 13^{\circ}\text{C}$) compared with 1980, and the bias of population growth towards hot places has the increased population density at the secondary ($\sim 27^{\circ}\text{C}$) peak. Greater observed global warming in the cooler higher northern latitudes than the tropics is visible in the changes to the distribution (Fig. 1a). Hot exposure (MAT $\geq 29^{\circ}\text{C}$) tripled in percentage terms to $0.9 \pm 0.4\%$ (mean \pm s.d.; 62 \pm 26 million people), 9 \pm 1% of the global population have been exposed outside the niche due to temperature change alone and 10 \pm 1% from temperature plus demographic change (Fig. 2). Thus, global warming of 0.7°C since 1960–1990 has put 624 \pm 70 million people in less favourable temperature conditions, with demographic change adding another 77 million.

Fig. 2: Population exposed outside of the temperature niche, following different SSPs.



Future exposure

To estimate future exposure, we use an ensemble of eight climate model outputs (Supplementary Table 1) and corresponding population projections from four Shared Socioeconomic Pathways⁵⁰ (SSPs; Extended Data Table 1)—scenarios of socioeconomic global changes and associated greenhouse gas emissions up to 2100. The ‘middle of the road’ (SSP2-4.5) pathway provides a useful reference scenario because it produces end-of-century (2081–2100) average global warming of 2.7 (range 2.1–3.5)°C corresponding to the 2.7 (2.0–3.6)°C expected under current policies¹, and it captures population growth towards a peak of ~9.5 billion in 2070 (then declining to ~9.0 billion in 2100). Global warming and population growth combine to shift relative population density to higher temperature (Fig. 1b). Hot exposure (Fig. 2a,d) becomes significant by 2030 at 4±2% or 0.3±0.1 billion as global warming reaches 1.5°C, and it increases near linearly to 23±9% or 2.1±0.8 billion in 2090 under 2.7°C global warming. The number of people left outside the niche due to temperature change alone (Fig. 2b,e) reaches 14±3% or 1.2±0.2 billion by 2030, more than doubling to 29±5% or 2.7±0.5 billion in 2090. The number of people left outside the niche from temperature plus demographic change (Fig. 2c,f) reaches 25±2% or 2.0±0.2 billion by 2030, and 40±4% or 3.7±0.4 billion by 2090.

Variation across the SSPs

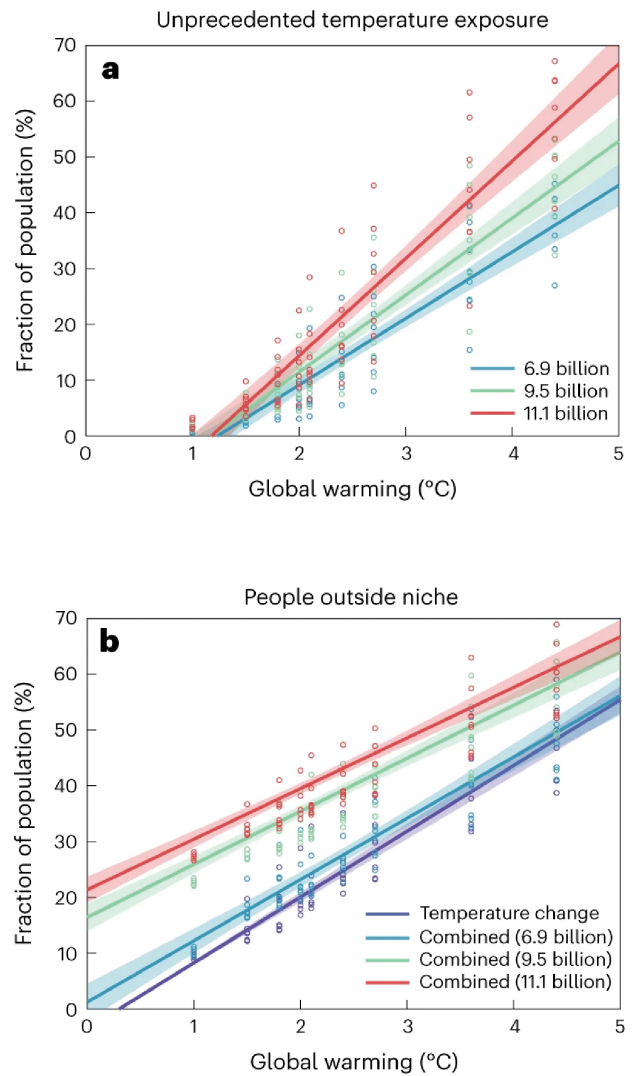
The other three SSPs produce a wide range of global warming (2081–2100) from ~1.8 (1.3–2.4)°C to ~4.4 (3.3–5.7)°C and span a wide range of human development trajectories, from population peaking at ~8.5 billion then declining to ~6.9 billion in 2100 to ongoing growth to ~12.6 billion in 2100 (Extended Data Table 1). Both global warming and demographic change alter the distribution of relative population density with respect to temperature (Extended Data Fig. 5). By 2090, hot exposure reaches 8–40% or 0.6–4.7 billion across scenarios (Fig. 2a,d). The number of people left outside the niche due to temperature change only reaches 18–47% or 1.3–4.7 billion (Fig. 2b,e). Adding in demographic change increases this to 29–53% or 2.2–6.5 billion (Fig. 2c,f). Estimates of exposure outside the combined temperature–precipitation niche are roughly 20% greater than for the temperature niche alone (Extended Data Fig. 6). The ‘fossil-fuelled development’ (SSP5-8.5) pathway exposes the greatest proportion of the population to unprecedented heat or being pushed out of the niche due to climate change alone, but the ‘regional rivalry’ (SSP3-7.0) pathway exposes the greatest proportion of the population due to climate and demographic change combined, and the greatest absolute numbers across all three measures of exposure (Fig. 2 and Extended Data Fig. 6).

a–f, Fraction of population (%; **a–c**) and absolute population (billion people; **d–f**) exposed to unprecedented temperatures (MAT $\geq 29^{\circ}\text{C}$; **a,d**), left outside the niche due to temperature change only (**b,e**) and left outside the niche due to temperature change and demographic change (**c,f**) for different SSPs. Calculations are based on MAT averaged over the 20-year intervals and population density distribution at the centre year of the corresponding intervals. Data are presented as mean values with the shaded regions corresponding to the 5th–95th percentiles.

Controlling for demography

Larger global populations following the SSPs place a greater proportion of people in hotter places, tending to leave more outside the niche (irrespective of global warming). To isolate the effects of climate policy and associated climate change on exposure, we fix the population and its distribution, exploring three different options: (1) 6.9 billion (as in 2010); (2) 9.5 billion (as in SSP2 in 2070); and (3) 11.1 billion (as in SSP3 in 2070). Having controlled for demography, global warming shifts the whole distribution of population density to higher temperatures (Fig. 1c and Extended Data Fig. 7). This results in linear relationships (Fig. 3) between global warming and the percentage of the population exposed to unprecedented heat or left outside the niche from temperature change only, or temperature change plus demographic change. Hot exposure (Fig. 3a) starts to become significant above the present level of $\sim 1.2^\circ\text{C}$ global warming and increases steeply at $11.9\% \text{ }^\circ\text{C}^{-1}$ (6.9 billion) to $17.5\% \text{ }^\circ\text{C}^{-1}$ (11.1 billion). Exposure due to temperature change alone increases $11.8\% \text{ }^\circ\text{C}^{-1}$ above the baseline defined at 0.3°C global warming (1960–1990; Fig. 3b). Factoring in demography, for a greater fixed population, the percent exposed is always greater, but the dependence on climate weakens somewhat towards $9.1\% \text{ }^\circ\text{C}^{-1}$ (for 11.1 billion). The relationships between global warming and exposure are all steeper for the temperature–precipitation niche (Extended Data Fig. 8a). The mean temperature experienced by an average person increases with global warming in a manner invariant to demography at $+1.5^\circ\text{C} \text{ }^\circ\text{C}^{-1}$ (Extended Data Fig. 8b), consistent with observations and models that the land warms ~ 1.5 times faster than the global average⁵¹.

Fig. 3: Relationships between global warming and population exposed outside the temperature niche for different fixed population distributions.



a, Population (%) exposed to unprecedented heat ($\text{MAT} \geq 29^\circ\text{C}$) for the different population distributions: 6.9 billion (blue; $n=65$, coefficient = $11.9\% \text{ }^\circ\text{C}^{-1}$, $r^2=0.83$); 9.5 billion (green; $n=65$, coefficient = $13.8\% \text{ }^\circ\text{C}^{-1}$, $r^2=0.83$); and 11.1 billion (red; $n=65$, coefficient = $17.5\% \text{ }^\circ\text{C}^{-1}$, $r^2=0.83$).

b, Population (%) exposed outside the temperature niche due to temperature change only (purple; $n=65$, coefficient = $11.8\% \text{ }^\circ\text{C}^{-1}$, forcing intercept at 1960–1990 global warming of 0.3°C), and due to the combined effects of temperature change and demographic change, for different fixed population distributions: 6.9 billion in 2010 (blue; $n=65$, coefficient = $11.0\% \text{ }^\circ\text{C}^{-1}$, $r^2=0.83$); 9.5 billion following SSP2 in 2070 (green; $n=65$, coefficient = $9.5\% \text{ }^\circ\text{C}^{-1}$, $r^2=0.84$); and 11.1 billion following SSP3 in 2070 (red; $n=65$, coefficient = $9.1\% \text{ }^\circ\text{C}^{-1}$, $r^2=0.84$). The shaded regions correspond to 95% two-sided confidence intervals of the estimated regression coefficients.

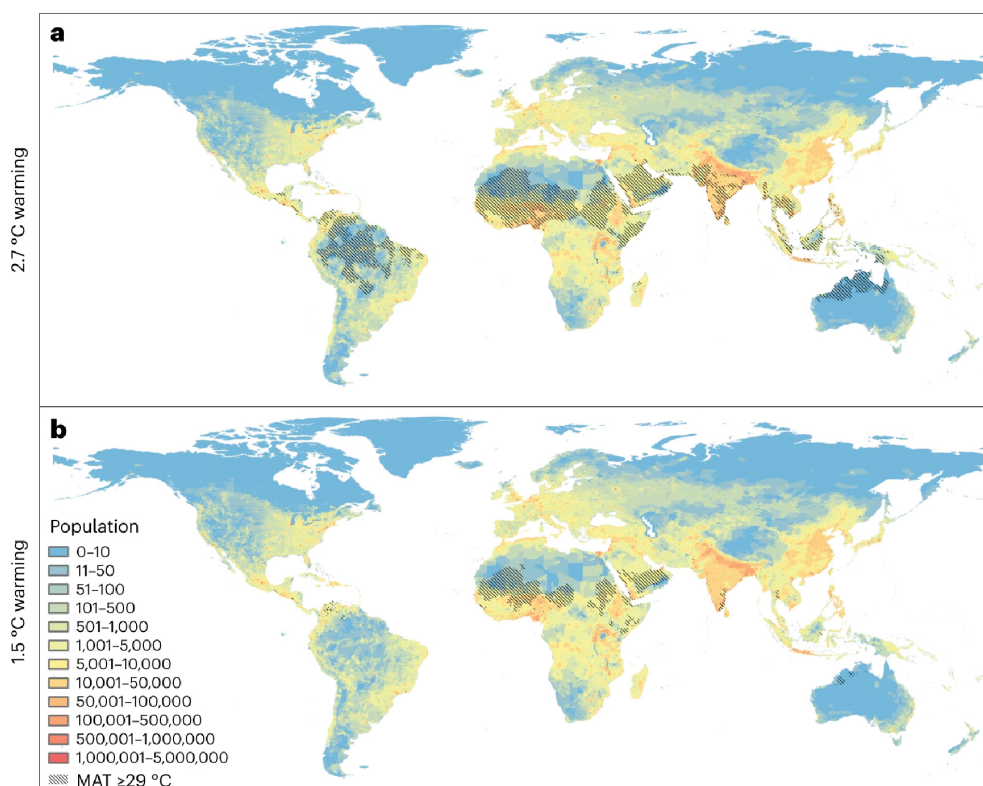
Worst-case scenarios

We now focus on a future world of 9.5 billion. When assessing risk it is important to consider worst-case scenarios⁵². If the transient climate response to cumulative emissions is high, current policies could, in the worst case, lead to $\sim 3.6^{\circ}\text{C}$ end-of-century global warming¹ (as projected under SSP3-7.0; Extended Data Table 1). This results in $34 \pm 10\%$ (3.3 ± 0.9 billion) hot exposed, $39 \pm 7\%$ (3.7 ± 0.7 billion) left outside the niche from temperature change only and $48 \pm 7\%$ (4.5 ± 0.6 billion) when including demographic change (Fig. 3). There also remains the possibility that climate policies are not enacted, and the world reverts to fossil-fuelled development (SSP5-8.5), leading to $\sim 4.4^{\circ}\text{C}$ end-of-century global warming. This gives $45 \pm 7\%$ (4.2 ± 0.7 billion) hot exposed, $47 \pm 8\%$ (4.5 ± 0.7 billion) left outside the niche from temperature change only and $55 \pm 7\%$ (5.3 ± 0.6 billion) when including demographic change (Fig. 3).

Gains from strengthening climate policy

Having controlled for demography, strengthening climate policy reduces exposure (Figs. 1c and 3), including to unprecedented heat (Fig. 4), through reducing geographical movement of the temperature and temperature–precipitation niches (Extended Data Fig. 9). Following Climate Action Tracker's November 2021 projections¹, different levels of policy ambition result in $\sim 0.3^{\circ}\text{C}$ changes in end-of-century global warming as follows: current policies lead to ~ 2.7 ($2.0\text{--}3.6$) $^{\circ}\text{C}$; meeting current 2030 nationally determined contributions (without long-term pledges) leads to ~ 2.4 ($1.9\text{--}3.0$) $^{\circ}\text{C}$; additional full implementation of submitted and binding long-term targets leads to ~ 2.1 ($1.7\text{--}2.6$) $^{\circ}\text{C}$; and fully implementing all announced targets leads to ~ 1.8 ($1.5\text{--}2.4$) $^{\circ}\text{C}$. Overall, going from $\sim 2.7^{\circ}\text{C}$ global warming under current policies to meeting the Paris Agreement 1.5°C target reduces hot exposure from 22 to 5% (2.1 to 0.4 billion; Fig. 3a). It reduces population left outside the niche due to temperature change only from 29 to 14% (2.8 to 1.3 billion) and it reduces population left outside the niche by temperature plus demographic changes from 39 to 28% (3.7 to 2.7 billion; Fig. 3b). Thus, each 0.3°C decline in end-of-century warming reduces hot exposure by 4.3% or 410 million people, it reduces population left outside the niche due to temperature change only by 3.7% or 350 million people, and population left outside the niche due to temperature and demographic changes by 2.8% or 270 million people.

Fig. 4: Regions and population densities exposed to unprecedented heat at different levels of global warming.

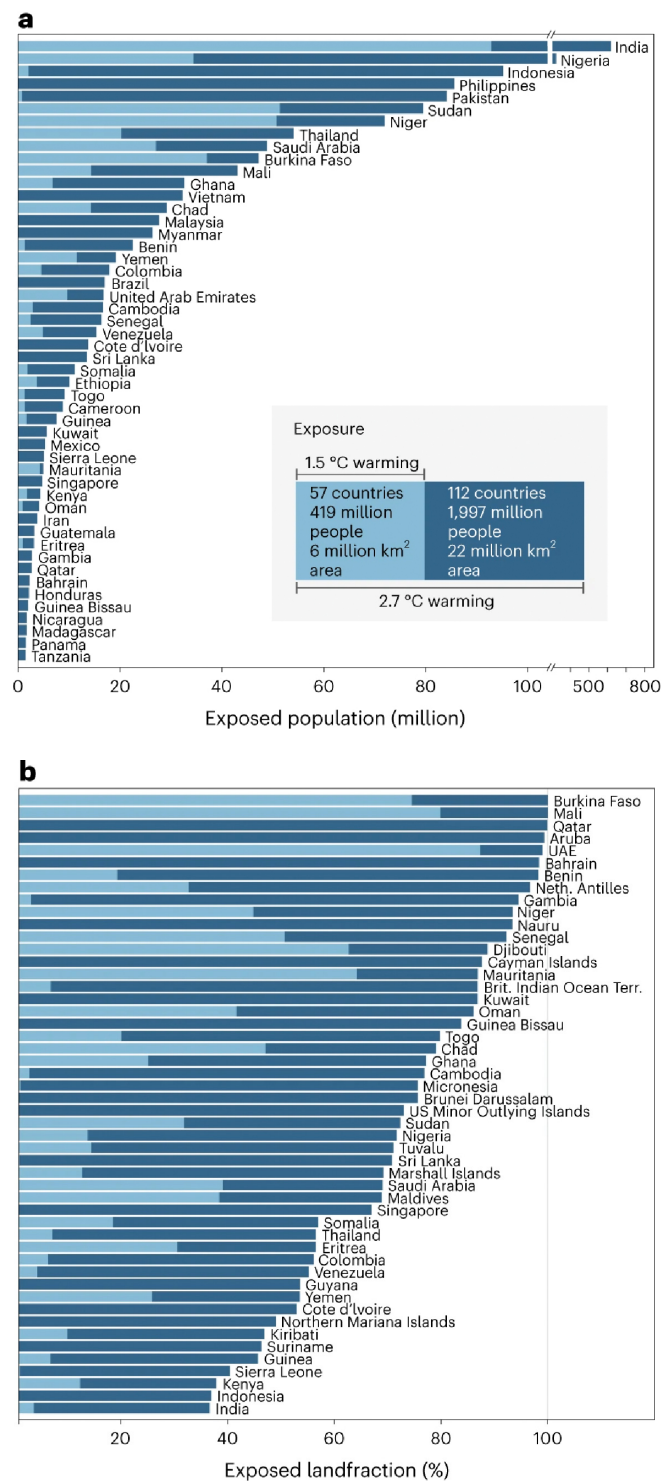


a,b, Regions exposed to unprecedented heat ($\text{MAT} \geq 29^{\circ}\text{C}$) overlaid on population density (number in a $\sim 100 \text{ km}^2$ grid cell) for a world of 9.5 billion (SSP2, 2070) under 2.7°C global warming (a) and 1.5°C global warming (b).

Country-level exposure

We focus on hot exposure as the simplest and most conservative metric. The population exposed to unprecedented heat ($\text{MAT} \geq 29^\circ\text{C}$) worldwide declines ~5-fold if global warming is reduced from $\sim 2.7^\circ\text{C}$ under current policies to meeting the 1.5°C target (Fig. 5a and Supplementary Data). Assuming a future world of 9.5 billion, India has the greatest population exposed under 2.7°C global warming, >600 million, but this reduces >6-fold to ~ 90 million at 1.5°C global warming. Nigeria has the second largest population exposed, >300 million under 2.7°C global warming, but this reduces >7-fold to <40 million at 1.5°C global warming. For third-ranked Indonesia, hot exposure reduces >20-fold, from ~ 100 million under 2.7°C global warming to <5 million at 1.5°C global warming. For fourth- and fifth-ranked Philippines and Pakistan with >80 million exposed under 2.7°C global warming, there are even larger proportional reductions at 1.5°C global warming. Sahelian–Saharan countries including Sudan (sixth ranked) and Niger (seventh) have a ~2-fold reduction in exposure, because they still have a large fraction of land area hot exposed at 1.5°C global warming (Fig. 5b). The fraction of land area exposed approaches 100% for several countries under 2.7°C global warming (Fig. 5b). Brazil has the greatest absolute land area exposed under 2.7°C global warming, despite almost no area being exposed at 1.5°C , and Australia and India also experience massive increases in absolute area exposed (Fig. 4). (If the future population reaches 11.1 billion, the ranking of countries by population exposed remains similar, although the numbers exposed increase.) Those most exposed under 2.7°C global warming come from nations that today are above the median poverty rate and below the median per capita emissions (Fig. 6).

Fig. 5: Country-level exposure to unprecedented heat ($\text{MAT} \geq 29^\circ\text{C}$) at 2.7°C and 1.5°C global warming in a world of 9.5 billion people (around 2070 under SSP2).



a, Population exposed for the top 50 countries ranked under 2.7°C global warming (dark blue) with exposure at 1.5°C global warming overlaid (pale blue). Note the break in the x axis for the top two countries.

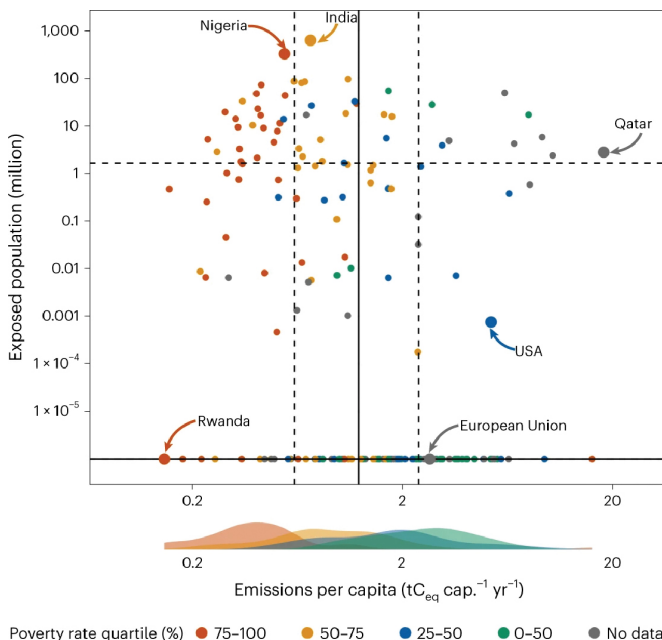
b, Fraction of land area exposed for the top 50 countries (again ranked under 2.7°C global warming with results for 1.5°C global warming overlaid). The inset in a summarizes the total global exposure of countries, population and land area at the two levels of global warming, with results for all countries provided in Supplementary Data. UAE, United Arab Emirates; Neth. Antilles, Netherlands Antilles; Brit. Indian Ocean Terr., British Indian Ocean Territory.

Relating present emissions to future exposure

Above the present level of 1.2°C global warming, the increase in hot exposure of $13.8\% \text{ }^{\circ}\text{C}^{-1}$ for a future world of ~ 9.5 billion people (cap.; Fig. 3a), corresponds to $1.31 \times 10^9 \text{ cap. } ^{\circ}\text{C}^{-1}$. The established relationship⁵³ of cumulative emissions (EgC) to transient global warming is ~ 1.65 ($1.0\text{--}2.3$) $^{\circ}\text{C}$ EgC $^{-1}$. Therefore one person will be exposed to unprecedented heat (MAT $\geq 29^{\circ}\text{C}$) for every ~ 460 ($330\text{--}760$) tC emitted. Present (2018 data) global mean per capita CO₂-equivalent (CeQ) emissions⁵⁴ (production-based) are $1.8 \text{ tCeQ cap.}^{-1} \text{ yr}^{-1}$. Thus, during their lifetimes (72.6 years) ~ 3.5 global average citizens today (less than the average household of 4.9 people) emit enough carbon to expose one future person to unprecedented heat. Citizens in richer countries generally have higher emissions⁵⁴, for example, the European Union ($2.4 \text{ tCeQ cap.}^{-1} \text{ yr}^{-1}$), the USA ($5.3 \text{ tCeQ cap.}^{-1} \text{ yr}^{-1}$) and

Qatar ($18 \text{ tCeQ cap.}^{-1} \text{ yr}^{-1}$; Fig. 6), and consumption-based emissions are even higher. Thus, ~ 2.7 average European Union citizens or ~ 1.2 average US citizens emit enough carbon in their lifetimes to expose one future person to unprecedented heat, and the average citizen of Qatar emits enough carbon in their lifetime to expose ~ 2.8 future people to unprecedented heat. Those future people tend to be in nations that today have per capita emissions around the 25% quantile (Fig. 6), including the two countries with the greatest population exposed: India ($0.73 \text{ tCeQ cap.}^{-1} \text{ yr}^{-1}$) and Nigeria ($0.55 \text{ tCeQ cap.}^{-1} \text{ yr}^{-1}$). We estimate that the average future person exposed to unprecedented heat comes from a place where today per capita emissions are approximately half (56%) of the global average (or 52% in a world of 11.1 billion people).

Fig. 6: Country-level per capita greenhouse gas emissions⁵⁴ related to population exposed to unprecedented heat (MAT $\geq 29^{\circ}\text{C}$) at 2.7°C global warming (Fig. 5a) and poverty rate⁸⁰.



Solid lines show the median (50% quantile) and dashed lines show the 25% and 75% quantiles for emissions and heat exposure. Points are coloured by quartile of the poverty rate distribution, where poverty rate is defined as the percentage of national population below the US\$1.90 poverty line. The density plots at the bottom show the distribution of emissions per capita for each poverty rate quartile.

Discussion

Our estimate that global warming since 1960–1990 has put more than 600 million people outside the temperature niche is consistent with attributable impacts of climate change affecting 85% of the world's population⁵⁵. Above the present level of $\sim 1.2^\circ\text{C}$ global warming, exposure to unprecedented average temperatures ($\text{MAT} \geq 29^\circ\text{C}$) is predicted to increase markedly (Fig. 3a), increasing exposure to temperature extremes (Extended Data Fig. 4). This is consistent with extreme humid heat having more than doubled in frequency⁴² since 1979, associated with labour loss of 148 million full-time equivalent jobs¹⁹, with exposure in urban areas increasing for 23% of the world's population⁵⁶ from 1983 to 2016 (due also to growing urban heat islands) and the total urban population exposed tripling⁵⁶ (due also to demographic change). Both India and Nigeria already show 'hotspots' of increased exposure to extreme heat due predominantly to warming⁵⁶, consistent with our prediction that they are at greatest future risk (Fig. 5). These and other emerging economies (for example, Indonesia, Pakistan, Thailand) dominate the total population exposed to unprecedented heat in a 2.7°C warmer world (Fig. 5). Their climate policy commitments also play a significant role in determining end-of-century global warming⁵.

The huge numbers of humans exposed outside the climate niche in our future projections warrant critical evaluation. Combined effects of temperature and demographic change are upper estimates. This is because at any given time the method limits absolute population density of the (currently secondary) higher-temperature peak based on absolute population density of the (currently primary) lower-temperature peak. Yet absolute population density is allowed to vary (everywhere) over time. (This is not an issue for the temperature change only or hot exposure estimates.) Nevertheless, a bias of population growth to hot places clearly increases the proportion (as well as the absolute number) of people exposed to harm from high temperatures⁵⁷. Colder places are projected to become more habitable (Extended Data Fig. 9) but are not where population growth is concentrated. Nor do we consider exposure to other sources of climate harm there (or elsewhere), including sea-level rise^{30,31}, increasing climate extremes⁵⁸ and permafrost thaw⁵⁹.

Overall, our results illustrate the huge potential human cost and the great inequity of climate change, informing discussions of loss and damage^{60,61}. The worst-case scenarios of $\sim 3.6^\circ\text{C}$ or even $\sim 4.4^\circ\text{C}$ global warming could put half of the world population outside the historical climate niche, posing an existential risk. The $\sim 2.7^\circ\text{C}$ global warming expected under current policies puts around a third of the world population outside the niche. It exposes almost the entire area of some countries (for example, Burkina Faso, Mali) to unprecedented heat, including some Small Island Developing States (for example, Aruba, Netherlands Antilles; Fig. 5b)—a group with members already facing an existential risk from sea-level rise. The gains from fully implementing all announced policy targets and limiting global warming to $\sim 1.8^\circ\text{C}$ are considerable, but would still leave nearly 10% of people exposed to unprecedented heat. Meeting the goal of the Paris Agreement to limit global warming to 1.5°C halves exposure outside the temperature niche relative to current policies and limits those exposed to unprecedented heat to 5% of people. This still leaves several least-developed countries (for example, Sudan, Niger, Burkina Faso, Mali) with large populations exposed (Fig. 5a), adding adaptation challenges to an existing climate investment trap⁶². Nevertheless, our results show the huge potential for more decisive climate policy to limit the human costs and inequities of climate change.

Methods

Reassessing the climate niche

We plot the running mean of population density against MAT, with a step of 1 °C and a bin size of 2 °C, and then apply double-Gaussian fitting to the resulting curve¹⁴. Our previous work¹⁴ assessed the human temperature niche by quantifying the 2015 population distribution in relation to the 1960–1990 MAT (Extended Data Fig. 1; ‘old reference’). Here, we re-assessed the temperature niche, changing the data to the 1980 population distribution (total 4.4 billion) under the 1960–1990 MAT, for greater internal consistency (Fig. 1a and Extended Data Fig. 1; ‘1980’). This is important because there has been significant population growth between 1980 and 2015 with a distinct bias to hotter places. The 1980 population distribution data were obtained from the History Database of the Global Environment (HYDE) 3.2 database⁶³. The ensemble mean 1960–1990 climate and associated uncertainty (5th/95th percentiles) were calculated from three sources: (1) WorldClim v.1.4 data⁶⁴; (2) Climate Research Unit Time Series (CRU TS) v.4.05 monthly data^{65,66}; and (3) National Aeronautics and Space Administration Global Land Data Assimilation System (NASA GLDAS-2.1) 3-hourly data⁶⁷. The revised temperature niche was compared with existing results for different historical intervals and datasets from ref. 14 (Extended Data Fig. 1). A revised temperature–precipitation niche was also calculated from both MAT and MAP, following the methods in ref. 14, but using the 1980 population distribution with the 1960–1990 mean climate.

Projecting the niche

Hot exposure is calculated (as previously¹⁴) for a given climate and population distribution as the percentage of people exposed to MAT ≥ 29 °C, from a direct spatial comparison of MAT and population distributions (without any smoothing). The MAT ≥ 29 °C threshold was chosen as only 0.3% of the 1980 population (12 million) experienced such conditions in the 1960–1990 climate. To separate the effects of climate and demographic changes on geographic displacement of the temperature niche (or the temperature–precipitation niche), we consider the following (Extended Data Fig. 3): (1) the geographic distribution of the reference niche (‘reference distribution’); (2) projecting the reference niche function to the geographic distribution of present/future climate (‘ideal distribution’); and (3) the geographically projected ‘assumed distribution’ of present/future population with respect to present/future climate conditions. Here, (2) minus (1) gives the effect of climate change only (as previously¹⁴), and (3) minus (2) gives the combined effect of climate and demographic change.

Linking average temperature to other thermal metrics

We assessed the relationships between MAT and other thermal metrics proposed to better capture thermal tolerance of humans, focusing on the recent interval 2000–2020. The correlations between MAT and annual MMT or mean annual WBT were assessed using linear regression with the ordinary least square method. MMT was calculated from the fifth generation European Centre for Medium-Range Weather Forecasts (ECMWF) reanalysis (ERA5) daily data at ~ 10 km spatial resolution and CRU TS v.4.06 monthly data at 0.5° spatial resolution. Mean annual WBT was calculated from ERA5 using the ‘one-third rule’ approximation based on a weighted average of dry-bulb and dewpoint temperatures⁶⁸ (this is reasonable for the annual average but overestimates daily maximum WBT). We used bias-corrected WBT⁶⁹ calculated from temperature and relative humidity data following the method of ref. 70 for six Coupled Model Intercomparison Project Phase 6 (CMIP6) models (limited to CNRM-CM6-1, CNRM-ESM2-1, CanESM5, GFDL-ESM4, MIROC-ES2L and MRI-ESM2-0 due to data availability) to derive daily maximum WBT and mean annual WBT. A model ensemble was created by resampling all model outputs to the coarsest model spatial resolution (2.8°; that of CanESM5 and GFDL-ESM4) using a bilinear interpolation method—each pixel in the resampled raster is the result of a weighted average of the nearest pixels in the original raster (this avoids biassing the ensemble towards higher resolution models). To assess the relationships between MAT and heat extremes, we considered the number of days with maximum temperature >40 °C or with WBT >28 °C. We used the ERA5 hourly data to calculate by grid point the average number of days in a year (between 2000 and 2020) with maximum dry-bulb temperature >40 °C. We used the CMIP6 model ensemble daily maximum WBT to calculate by grid point the average number of days per year (between 2000 and 2020) with maximum WBT >28 °C. Running means were calculated with a bin width of 2 °C, a step of 0.5 °C and a minimum bin size of 20 data points.

Changes up to present

To calculate changes up to (near) present, we construct an ensemble mean 2000–2020 climate and associated uncertainty (5th/95th percentiles) from five sources: (1) CRU TS v.4.05 monthly data^{65,66}; (2) NASA GLDAS-2.1 3-hourly data⁶⁷; (3) ECMWF ERA5-Land monthly averaged climate reanalysis data⁷¹; (4) NASA Famine Early Warning Systems Network Land Data Assimilation System (FLDAS) monthly data^{72,73}; and (5) the United States National Centers for Environmental Prediction Climate Forecast System Version 2 (NCEP CFSv2) 6-hourly data⁷⁴. Each climate dataset is aggregated to calculate MAT and precipitation. The 2000–2020 climate represents 1.0°C global warming relative to the pre-industrial level. The 2010 population distribution data was obtained from the HYDE 3.2 database⁶³. We followed the methods described above to calculate exposure.

Future projections

We used projected climate and population distribution under four different SSPs, which combine different demographic⁷⁵ and emissions projections under consistent storylines: SSP1-2.6 (sustainability), SSP2-4.5 (middle of the road), SSP3-7.0 (regional rivalry) and SSP5-8.5 (fossil-fuelled development). We focused on 20-year mean climate states for 2020–2040, 2040–2060, 2060–2080 and 2080–2100, and the projected population distribution data of 2030, 2050, 2070 and 2090, to represent average demographic conditions of corresponding time periods (Extended Data Table 1). We obtained downscaled CMIP6 climate data available from WorldClim v.2.0 at 0.0833° (~10 km) resolution, which restricts us to up to eight CMIP6 models: BCC-CSM2-MR, CNRM-CM6-1, CNRM-ESM2-1, CanESM5, GFDL-ESM4, IPSL-CM6A-LR, MIROC-ES2L and MRI-ESM2-0 (Supplementary Table 1). We obtained SSP population projection data at 1 km resolution from the spatial population scenarios dataset^{76,77}. The SSP population projections were derived at national level using methods of multi-dimensional mathematical demography⁷⁵. Alternative assumptions on future fertility, mortality, migration and educational transitions align to the SSP storylines on future development⁷⁸ (and exclude climate-induced migration). Spatially explicit data in line with those country-level projections were derived at 1/8° resolution using a parameterized gravity-based downscaling model⁷⁶, and further downscaled to 1 km resolution⁷⁷. We aggregated this population data to a consistent resolution of 0.0833° (~10 km) to match the climate data and our previous analyses. We combine results across climate models to create a multi-model ensemble mean, and a 5–95% confidence interval, recognizing that the number of models available varies somewhat between SSPs and time-slices (Supplementary Table 1). To this end, we apply the MAT data of each climate model to plot population density against MAT and then combine the resulting curves to calculate the mean, and 5th and 95th percentiles.

Controlling for demography

To control for demography and thus isolate the effects of climate policy and associated climate change on exposure, we consider three different fixed populations and their spatial distributions: (1) 6.9 billion as in 2010; (2) 9.5 billion following SSP2 in 2070^{75,76,77}; and (3) 11.1 billion following SSP3 in 2070^{75,76,77}. These are combined with the observed (2000–2020) 1.0°C global warming and with different future levels of global warming (1.5, 1.8, 2.0, 2.1, 2.4, 2.7, 3.6 and 4.4°C) corresponding to different 20-year climate averages from different SSPs (Figs. 1c and 3, and Extended Data Fig. 7). Global warming of 1.5°C and 2.0°C are considered because of their relevance to the Paris Agreement. Values of 1.8, 2.1, 2.4 and 2.7°C are chosen as best estimates of end-of-century global warming corresponding to different policy assumptions, taken from the Climate Action Tracker¹, which uses an ensemble of runs of the MAGICC6 model that, in turn, emulates different general circulation models from CMIP6. Global warming values of 3.6 and 4.4°C are chosen as worst-case scenarios that also enable examining the shape of relationships between global warming and population exposure. Twenty-year SSP intervals corresponding to these different levels of global warming are chosen based on mean global warming levels from the CMIP6 model ensemble given in Table SPM.1 of the Sixth Assessment Report (AR6) of the Intergovernmental Panel on Climate Change⁷⁹ (IPCC). We try to match to warming in 2081–2100, but where earlier time intervals must be used this should have little effect on the results because the spatial pattern of temperature change is highly conserved on the century timescale. The different combinations are: 1.5°C=SSP1-2.6 in 2021–2040; 1.8°C=SSP1-2.6 in 2081–2100; 2.0°C=SSP2-4.5 in 2041–2060; 2.1°C=SSP3-7.0 in 2041–2060; 2.4°C=SSP5-8.5 in 2041–2060; 2.7°C=SSP2-4.5 in 2081–2100; 3.6°C=SSP3-7.0 in 2081–2100; and 4.4°C=SSP5-8.5 in 2081–2100. For the same time interval and SSP, different CMIP6 models can give different levels of global warming due to differing climate sensitivity. This is apparent in the spread of population exposure results for individual models (open circles in Fig. 3; Extended Data Fig. 8). However, we checked that global warming in the multi-model ensemble mean of the CMIP6 models we consider (Supplementary Table 1) matches that of the larger CMIP6 ensemble (Table SPM.1 of IPCC AR6).

Country-level estimates

Results for hot exposure for 2.7°C and 1.5°C global warming and populations of 9.5 or 11.1 billion were aggregated from the 0.0833° (~10km) scale of the population and climate data to country scale. This summed the population in all grid cells within a country boundary where $\text{MAT} \geq 29^\circ\text{C}$, using geographic information system data for country boundaries from the World Borders Dataset. For the grid cells that are intersected by a country boundary, they were associated with a country if over half the grid cell area fell within the country territory. Results for all countries are given in Supplementary Data.

Emissions and poverty rate of those exposed

Using the country-level breakdown of exposure to unprecedented heat in a 2.7°C warmer world with 9.5 billion people (Fig. 5a and Supplementary Data), we calculated a weighted average for number of people exposed multiplied by percentage of global average emissions per capita today. This uses production-based, country-level Ceq greenhouse gas emissions from the emissions database for global atmospheric research⁵⁴, for which 2018 is the latest year. The calculation was also done for country-level exposure in a 2.7°C warmer world of 11.1 billion. Consumption-based emissions (accounting for trade) tend to be lower than production-based emissions in poorer countries and higher in richer countries. This would increase the inequity already apparent in the results. We also examined poverty rate defined as the percentage of population per country below the US\$1.90 poverty line, using the interpolated data for 2019 from the World Bank's Poverty and Inequality Platform⁸⁰. The resulting distribution is heavily skewed with 25% quantile = 0.26%, 50% quantile = 1.79% and 75% quantile = 20%.

References

1. *Climate Action Tracker: Warming Projections Global Update: November 2021* (Climate Analytics & NewClimate Institute, 2021)
2. *World Energy Outlook 2021* (International Energy Agency, 2021).
3. *Emissions Gap Report 2021: The Heat Is On—A World of Climate Promises Not Yet Delivered* (United Nations Environment Programme, 2021)
4. *Addendum to the Emissions Gap Report 2021* (United Nations Environment Programme, 2021)
5. Meinshausen, M. et al. Realization of Paris Agreement pledges may limit warming just below 2°C. *Nature* 604, 304–309 (2022)
6. Newell, P., Srivastava, S., Naess, L. O., Torres Contreras, G. A. & Price, R. Toward transformative climate justice: an emerging research agenda. *Wiley Interdiscip. Rev. Clim. Change* 12, e733 (2021)
7. Nordhaus, W. D. Revisiting the social cost of carbon. *Proc. Natl Acad. Sci. USA* 114, 1518–1523 (2017)
8. Nolt, J. Casualties as a moral measure of climate change. *Clim. Change* 130, 347–358 (2015)
9. Watts, N. et al. The 2020 report of The Lancet Countdown on health and climate change: responding to converging crises. *Lancet* 397, 129–170 (2021)
10. Guo, Y. et al. Global variation in the effects of ambient temperature on mortality: a systematic evaluation. *Epidemiology* 25, 781–789 (2014)
11. Gasparrini, A. et al. Mortality risk attributable to high and low ambient temperature: a multicountry observational study. *Lancet* 386, 369–375 (2015)
12. Mora, C. et al. Global risk of deadly heat. *Nat. Clim. Change* 7, 501–506 (2017)
13. Parncutt, R. The human cost of anthropogenic global warming: semi-quantitative prediction and the 1,000-tonne rule. *Front. Psychol.* (2019)
14. Xu, C., Kohler, T. A., Lenton, T. M., Svenning, J.-C. & Scheffer, M. Future of the human climate niche. *Proc. Natl Acad. Sci. USA* 117, 11350–11355 (2020)
15. Pörtner, H.-O. Climate impacts on organisms, ecosystems and human societies: integrating OCLTT into a wider context. *J. Exp. Biol.* (2021)
16. Lutterschmidt, W. I. & Hutchison, V. H. The critical thermal maximum: history and critique. *Can. J. Zool.* 75, 1561–1574 (1997)
17. Afkhami, M. E., McIntyre, P. J. & Strauss, S. Y. Mutualist-mediated effects on species' range limits across large geographic scales. *Ecol. Lett.* 17, 1265–1273 (2014)
18. Burke, M., Hsiang, S. M. & Miguel, E. Global non-linear effect of temperature on economic production. *Nature* 527, 235–239 (2015)
19. Parsons, L. A. et al. Global labor loss due to humid heat exposure underestimated for outdoor workers. *Environ. Res. Lett.* 17, 014050 (2022)
20. Masuda, Y. J. et al. Heat exposure from tropical deforestation decreases cognitive performance of rural workers: an experimental study. *Environ. Res. Lett.* 15, 124015 (2020)
21. Park, R. J., Behrer, A. P. & Goodman, J. Learning is inhibited by heat exposure, both internationally and within the United States. *Nat. Hum. Behav.* 5, 19–27 (2021)
22. Chersich, M. F. et al. Associations between high temperatures in pregnancy and risk of preterm birth, low birth weight, and stillbirths: systematic review and meta-analysis. *Br. Med. J.* 371, m3811 (2020)
23. Mares, D. M. & Moffett, K. W. Climate change and interpersonal violence: a “global” estimate and regional inequities. *Clim. Change* 135, 297–310 (2016)
24. Hsiang, S. M., Burke, M. & Miguel, E. Quantifying the influence of climate on human conflict. *Science* 341, 1235367 (2013).
25. Hsiang, S. M., Meng, K. C. & Cane, M. A. Civil conflicts are associated with the global climate. *Nature* 476, 438–441 (2011)
26. Stechemesser, A., Levermann, A. & Wenz, L. Temperature impacts on hate speech online: evidence from 4 billion geolocated tweets from the USA. *Lancet Planet. Health* 6, e714–e725 (2022)
27. Mueller, V., Gray, C. & Kosec, K. Heat stress increases long-term human migration in rural Pakistan. *Nat. Clim. Change* 4, 182–185 (2014)
28. Cissé, G. et al. in *Climate Change 2022: Impacts, Adaptation and Vulnerability* (eds Pörtner, H.-O. et al.) 1041–1170 (IPCC, Cambridge Univ. Press, 2022)
29. Carlson, C. J. et al. Climate change increases cross-species viral transmission risk. *Nature* 607, 555–562 (2022)
30. Neumann, B., Vafeidis, A. T., Zimmermann, J. & Nicholls, R. J. Future coastal population growth and exposure to sea-level rise and coastal flooding—a global assessment. *PLoS ONE* 10, e0118571 (2015)
31. Hooijer, A. & Vernimmen, R. Global LiDAR land elevation data reveal greatest sea-level rise vulnerability in the tropics. *Nat. Commun.* 12, 3592 (2021)
32. Small, C. & Cohen, J. Continental physiography, climate, and the global distribution of human population. *Curr. Anthropol.* 45, 269–277 (2004)
33. Gavin, M. C. et al. The global geography of human subsistence. *R. Soc. Open Sci.* 5, 171897 (2018)
34. Pitulko, V. V. et al. The Yana RHS site: humans in the Arctic before the Last Glacial Maximum. *Science* 303, 52–56 (2004)
35. Pitulko, V., Pavlova, E. & Nikolskiy, P. Revising the archaeological record of the Upper Pleistocene Arctic Siberia: human dispersal and adaptations in MIS 3 and 2. *Quat. Sci. Rev.* 165, 127–148 (2017)
36. Taylor, W. et al. High altitude hunting, climate change, and pastoral resilience in eastern Eurasia. *Sci. Rep.* 11, 14287 (2021)
37. Just, M. G., Nichols, L. M. & Dunn, R. R. Human indoor climate preferences approximate specific geographies. *R. Soc. Open Sci.* 6, 180695 (2019)

38. Cui, W., Cao, G., Park, J. H., Ouyang, Q. & Zhu, Y. Influence of indoor air temperature on human thermal comfort, motivation and performance. *Build. Environ.* 68, 114–122 (2013)

39. Masuda, Y. J. et al. How are healthy, working populations affected by increasing temperatures in the tropics? Implications for climate change adaptation policies. *Glob. Environ. Change* 56, 29–40 (2019)

40. Asseng, S., Spänkuch, D., Hernandez-Ochoa, I. M. & Laporta, J. The upper temperature thresholds of life. *Lancet Planet. Health* 5, e378–e385 (2021).

41. Sherwood, S. C. & Huber, M. An adaptability limit to climate change due to heat stress. *Proc. Natl Acad. Sci. USA* 107, 9552–9555 (2010)

42. Raymond, C., Matthews, T. & Horton, R. M. The emergence of heat and humidity too severe for human tolerance. *Sci. Adv.* 6, eaaw1838 (2020)

43. Weitz, C. A., Mukhopadhyay, B. & Das, K. Individually experienced heat stress among elderly residents of an urban slum and rural village in India. *Int. J. Biometeorol.* 66, 1145–1162 (2022)

44. Dunn, R. R., Davies, T. J., Harris, N. C. & Gavin, M. C. Global drivers of human pathogen richness and prevalence. *Proc. R. Soc. B* 277, 2587–2595 (2010)

45. Kummu, M., de Moel, H., Ward, P. J. & Varis, O. How close do we live to water? A global analysis of population distance to freshwater bodies. *PLoS ONE* 6, e20578 (2011)

46. Bennett, J. M. et al. GlobTherm, a global database on thermal tolerances for aquatic and terrestrial organisms. *Sci. Data* 5, 180022 (2018)

47. Bebber, D. P., Ramotowski, M. A. T. & Gurr, S. J. Crop pests and pathogens move polewards in a warming world. *Nat. Clim. Change* 3, 985–988 (2013)

48. Chaloner, T. M., Gurr, S. J. & Bebber, D. P. Plant pathogen infection risk tracks global crop yields under climate change. *Nat. Clim. Change* 11, 710–715 (2021)

49. Sloat, L. L. et al. Climate adaptation by crop migration. *Nat. Commun.* 11, 1243 (2020)

50. Riahi, K. et al. The Shared Socioeconomic Pathways and their energy, land use, and greenhouse gas emissions implications: an overview. *Glob. Environ. Change* 42, 153–168 (2017)

51. Lambert, F. H. & Chiang, J. C. H. Control of land-ocean temperature contrast by ocean heat uptake. *Geophys. Res. Lett.* 34, L13704 (2007)

52. Kemp, L. et al. Climate endgame: exploring catastrophic climate change scenarios. *Proc. Natl Acad. Sci. USA* 119, e2108146119 (2022)

53. Canadell, J. G. et al. in *Climate Change 2021: The Physical Science Basis* (eds Masson-Delmotte, V. et al.) 673–816 (IPCC, Cambridge Univ. Press, 2021)

54. Crippa, M. et al. *Emissions Database for Global Atmospheric Research, Version v6.0_FT_2020 (GHG Time-Series)* (European Commission, Joint Research Centre, 2021)

55. Callaghan, M. et al. Machine-learning-based evidence and attribution mapping of 100,000 climate impact studies. *Nat. Clim. Change* 11, 966–972 (2021)

56. Tuholske, C. et al. Global urban population exposure to extreme heat. *Proc. Natl Acad. Sci. USA* 118, e2024792118 (2021)

57. Klein, T. & Anderegg, W. R. L. A vast increase in heat exposure in the 21st century is driven by global warming and urban population growth. *Sustain. Cities Soc.* 73, 103098 (2021)

58. Seneviratne, S. I. et al. in *Climate Change 2021: The Physical Science Basis* (eds Masson-Delmotte, V. et al.) 1513–1766 (IPCC, Cambridge Univ. Press, 2021)

59. Ramage, J. et al. Population living on permafrost in the Arctic. *Popul. Environ.* 43, 22–38 (2021)

60. McNamara, K. E. & Jackson, G. Loss and damage: a review of the literature and directions for future research. *Wiley Interdiscip. Rev. Clim. Change* 10, e564 (2019)

61. New, M. et al. in *Climate Change 2022: Impacts, Adaptation and Vulnerability* (eds Pörtner, H.-O. et al.) 2539–2654 (IPCC, Cambridge Univ. Press, 2022).

62. Ameli, N. et al. Higher cost of finance exacerbates a climate investment trap in developing economies. *Nat. Commun.* 12, 4046 (2021)

63. Klein Goldewijk, K., Beusen, A., Doelman, J. & Stehfest, E. Anthropogenic land use estimates for the Holocene – HYDE 3.2. *Earth Syst. Sci. Data* 9, 927–953 (2017)

64. Hijmans, R. J., Cameron, S. E., Parra, J. L., Jones, P. G. & Jarvis, A. Very high resolution interpolated climate surfaces for global land areas. *Int. J. Climatol.* 25, 1965–1978 (2005)

65. Harris, I., Osborn, T. J., Jones, P. & Lister, D. Version 4 of the CRU TS monthly high-resolution gridded multivariate climate dataset. *Sci. Data* 7, 109 (2020)

66. University of East Anglia Climatic Research Unit; Harris, I. C., Jones, P. D. & Osborn, T. CRU TS4.05: Climatic Research Unit (CRU) Time-Series (TS) Version 4.05 of High-Resolution Gridded Data of Month-by-Month Variation in Climate (Jan. 1901–Dec. 2020) (NERC EDS Centre for Environmental Data Analysis, 2021)

67. Rodell, M. et al. The Global Land Data Assimilation System. *Bull. Am. Meteorol. Soc.* 85, 381–394 (2004)

68. Knox, J. A., Nevius, D. S. & Knox, P. N. Two simple and accurate approximations for wet-bulb temperature in moist conditions, with forecasting applications. *Bull. Am. Meteorol. Soc.* 98, 1897–1906 (2017)

69. Sandstad, M., Schwingshackl, C., Illes, C. E. & Sillmann, J. *Climate Extreme Indices and Heat Stress Indicators Derived from CMIP6 Global Climate Projections* (Copernicus Climate Change Service Climate Data Store, accessed 26 October 2022)

70. Buzan, J. R., Oleson, K. & Huber, M. Implementation and comparison of a suite of heat stress metrics within the Community Land Model version 4.5. *Geosci. Model Dev.* 8, 151–170 (2015)

71. Muñoz Sabater, J. *ERA5-Land Monthly Averaged Data From 1950 to Present* (Copernicus Climate Change Service Climate Data Store, accessed 3 May 2022)

72. McNally, A. et al. A land data assimilation system for sub-Saharan Africa food and water security applications. *Sci. Data* 4, 170012 (2017)

73. McNally, A. NASA/GSFC/HSL FLDAS Noah Land Surface Model L4 Global Monthly 0.1 x 0.1 Degree (MERRA-2 and CHIRPS) (Goddard Earth Sciences Data and Information Services Center, accessed 3 May 2022)

74. Saha, S. et al. *NCEP Climate Forecast System Version 2 (CFSv2) 6-Hourly Products* (Research Data Archive at the National Center for Atmospheric Research, Computational and Information Systems Laboratory, 2011)

75. KC, S. & Lutz, W. The human core of the Shared Socioeconomic Pathways: population scenarios by age, sex and level of education for all countries to 2100. *Glob. Environ. Change* 42, 181–192 (2017)

76. Jones, B. & O'Neill, B. C. Spatially explicit global population scenarios consistent with the Shared Socioeconomic Pathways. *Environ. Res. Lett.* 11, 084003 (2016)

77. Gao, J. *Downscaling Global Spatial Population Projections from 1/8-Degree to 1-km Grid Cells* (No. NCAR/TN-537+STR) (National Center for Atmospheric Research, Technical Notes, 2017)

78. O'Neill, B. C. et al. A new scenario framework for climate change research: the concept of Shared Socioeconomic Pathways. *Clim. Change* 122, 387–400 (2014)

79. IPCC in *Climate Change 2021: The Physical Science Basis* (eds Masson-Delmotte, V. et al.) 3–32 (Cambridge Univ. Press, 2021)

80. *Poverty and Inequality Platform* (World Bank, accessed 20 May 2022)

Acknowledgements

We thank all the data providers. T.M.L., J.F.A. and A.G. are supported by the Open Society Foundations (OR2021-82956). T.M.L. is supported by a Turing Fellowship. C.X. is supported by the National Key R&D Program of China (2022YFF1301000), the National Natural Science Foundation of China (32061143014) and the Fundamental Research Funds for the Central Universities (9610065). J.-C.S. is supported by VILLUM Investigator project ‘Biodiversity Dynamics in a Changing World’ funded by VILLUM FONDEN (grant 16549). M.S. is supported by an ERC Advanced Grant and a Spinoza award. This work is part of the Earth Commission, which is hosted by Future Earth and is the science component of the Global Commons Alliance. The Global Commons Alliance is a sponsored project of Rockefeller Philanthropy Advisors, with support from Oak Foundation, MAVA, Porticus, Gordon and Betty Moore Foundation, Herlin Foundation and the Global Environment Facility.

Author information

These authors contributed equally: Timothy M. Lenton, Chi Xu.

Authors and Affiliations

Global Systems Institute, University of Exeter, Exeter, UK
Timothy M. Lenton, Jesse F. Abrams & Ashish Ghadiali

School of Life Sciences, Nanjing University, Nanjing, China
Chi Xu

Potsdam Institute for Climate Impact Research, Potsdam, Germany
Sina Loriani & Boris Sakschewski

International Institute for Applied Systems Analysis, Laxenburg, Austria
Caroline Zimm

Center for Health and the Global Environment, University of Washington, Seattle, WA, USA
Kristie L. Ebi

Department of Applied Ecology, North Carolina State University, Raleigh, NC, USA
Robert R. Dunn

Center for Biodiversity Dynamics in a Changing World (BIOCHANGE) and Section for Ecoinformatics and Biodiversity, Department of Biology, Aarhus University, Aarhus, Denmark
Jens-Christian Svenning

Wageningen University, Wageningen, The Netherlands
Marten Scheffer

Contributions

T.M.L., C.X. and M.S. designed the study. C.X. performed the climate niche analyses with input from T.M.L. T.M.L. and J.F.A. related present emissions to future exposure. C.X., J.F.A. and S.L. produced the figures with input from T.M.L., B.S. and C.Z. T.M.L. wrote the paper with input from C.X., J.F.A., A.G., S.L., B.S., C.Z., K.L.E., R.R.D., J.-C.S. and M.S.

Corresponding authors

Correspondence to Timothy M. Lenton or Chi Xu.

*RADICAL
ECOLOGY*